Different types of chaos in optically injected semiconductor lasers

Bernd Krauskopf [a], Sebastian Wieczorek [b], and Daan Lenstra [b]

[a] *Dept of Engineering Mathematics, University of Bristol, Bristol BS8 1TR, UK*
[b] *Department of Physics and Astronomy, Vrije Universiteit Amsterdam, De Boelelaan 1081, 1081 HV Amsterdam, The Netherlands*

April 14, 2000

We present a detailed study of chaos in an optically injected semiconductor laser. Advanced tools from bifurcation theory are employed to identify routes to chaos via period-doublings and the break-up of different tori. This allows us to distinguish between different types of chaos in terms of the output characteristics of the laser. We also find locking to a periodic solution inside a region of chaos. This information is important for applications requiring chaotic signals, such as encryption schemes.

As complex nonlinear dynamics are of increasing interest for applications, such as cryptography[1,2] and computing[3], the question arises to locate and study sources of chaotic output. Laser systems are natural candidates because they are indeed known to produce chaotic output and have the additional advantage of operating on very short time scales. Arguably the most accessible such laser system is a semiconductor laser subject to external optical injection[4]. It is known that optical injection produces an enormous variety of phenomena, including chaotic output[5–10].

An optically injected semiconductor laser is described well by the *three-dimensional* single-mode rate equation model[4,10]

$$\dot{E} = K + \left(\frac{1}{2}(1+i\alpha)n - i\omega\right) E \qquad (1)$$
$$\dot{n} = -2\Gamma n - (1+2Bn)(|E|^2 - 1) \ .$$

Here E is the complex electric field, n is the population inversion, K is the injected field strength, and ω the detuning of the injected field from the solitary laser frequency. Furthermore, α is the linewidth enhancement factor, B is the cavity life time, and Γ is the damping rate. To keep this exposition simple we restrict to the case $\alpha = 2$, but similar routes to chaos are present for different results are α-values[10]. Furthermore, we set $B = 0.015$ and $\Gamma = 0.035$.

To find and distinguish between different types of chaos we take the point of view of bifurcation theory and find and continue bifurcation curves of Eqns. (1) in the (K, ω)-plane[10]. The resulting bifurcation diagram is shown in Fig. 1. Presented are saddle-node bifurcations (SN), Hopf bifurcations (H), period-doubling bifurcations (PD), saddle-node of limit cycle bifurcations (SL), and torus bifurcations (T). Supercritical bifurcations of stable objects are in black, and subcritical bifurcations of unstable objects are in grey. Superscripts in the labeling distinguish between bifurcation curves of periodic orbits of basic period and those that have already undergone a period-doubling. We remark, that we only show the bifurcation curves that are relevant here to avoid overcrowding in Fig. 1. This bifurcation diagram is in good agreement with experimental and numerical studies[8,9]. At the same time it shows more detail, which allows us to study different transitions to different types of chaos.

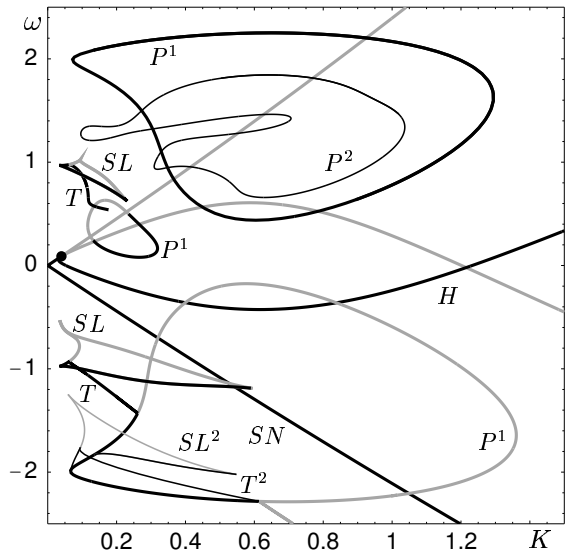

Fig. 1. The bifurcation diagram in the (K, ω)-plane.

To examine these transitions in terms of the output characteristics of the laser we take cross sections through the bifurcation diagram in Fig. 1 and present the respective dynamics in four columns showing: the three-dimensional attractor of Eqns. (1) projected onto the complex E-plane, the attractor of the corresponding Poincaré map, the time series of the power, and the optical spectrum.

First we illustrate in Fig. 2 the well-known period-doubling route to chaos with a vertical cross section through the nested islands of period-doublings in Fig. 1. An attracting periodic orbit (a) undergoes a sequence

of period-doublings (b)-(d) until it apparently becomes chaotic (e) and (f). This is very clear in the attractors of the Poincaré map, the power series, and the spectra. Notice that the attractor in (e) is already chaotic, but that it shows the typical almost one-dimensional shape of an attractor that appears after successive period-doublings. Large peaks are present in the spectrum, so that it is hard to decide whether the spectrum is already broad. The attractor then grows further (f) into a shape that is not immediately recognizable as an attractor coming from a transition via period-doublings. The spectrum becomes broader and the period-doubling peaks are less prominent, but still present.

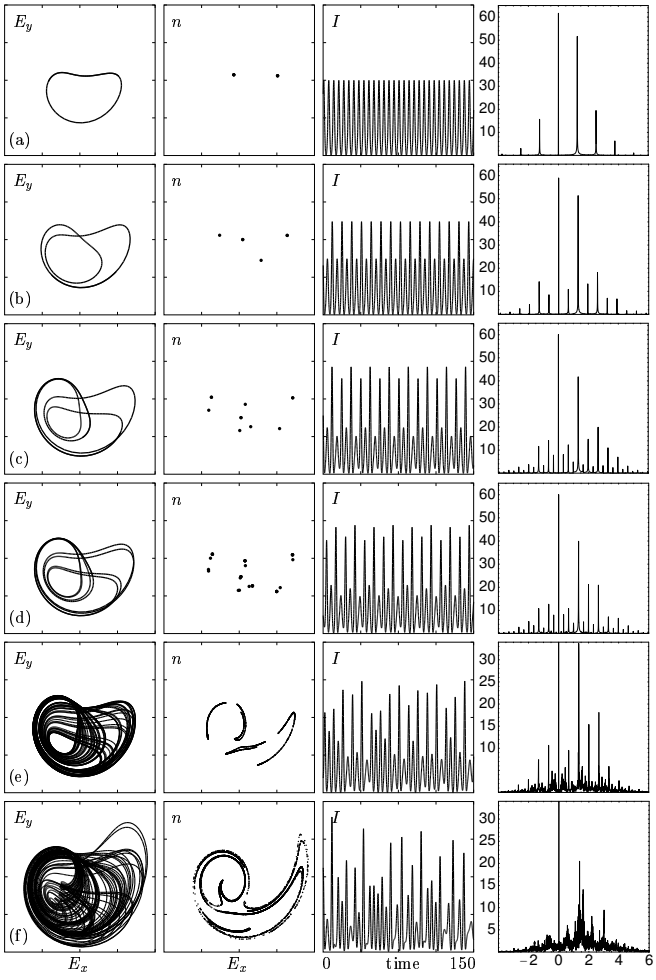

Fig. 2. Period-doubling route to chaos; $K = 0.62$ and from (a) to (f) ω takes the values 0.3, 0.5, 0.7, 0.71, 0.78, and 1.1.

An entirely different route to chaos is that via the break-up of a torus in Fig. 3. An attracting periodic orbit (a) loses its stability and a smooth attracting torus with quasiperiodic motion appears (b). This can also be seen in the power series and in the spectrum. Motion on a torus can be quasiperiodic or locked, and this is governed by resonance tongues. In general, a torus starts to break up when it is followed into a region where resonance tongues overlap.

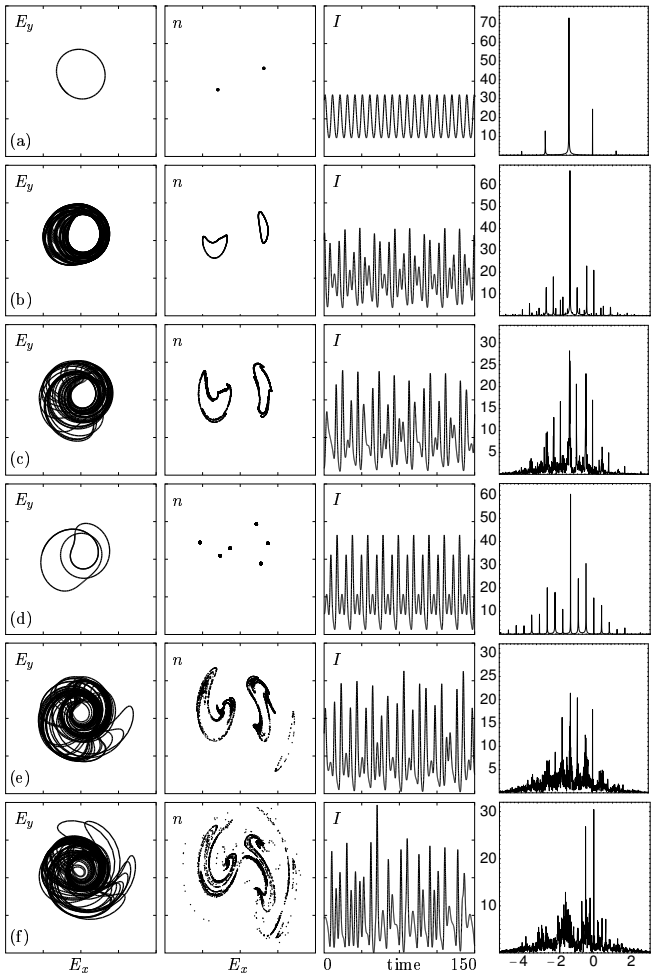

Fig. 3. Transition to chaos via the break-up of a torus; $\omega = -1.2$ and from (a) to (f) K takes the values 0.15, 0.19, 0.23, 0.25, 0.29 and 0.44.

The smooth torus in (b) starts to lose its smoothness by forming self-similar protrusions (c) forming a chaotic attractor as is evidenced by the fractal structure of the attractor of the Poincaré map, which nevertheless still is close to the original smooth torus. Also in the spectrum, which is broad, there is still much left of the previous dynamics. An important feature we found is locking on this chaotic attractor. There is a window where there is no chaotic dynamics observable in the system. Instead we find locking onto a period-three orbit (d): the power series is periodic with respective peaks in the spectrum. When the parameter is changed further the chaotic attractor reappears (e) and it becomes bigger (f) and does not resemble the original torus any longer. This can also be seen in the spectrum, which broadens considerably (e) and then also looses the typical peaks of the torus

dynamics (f). This transition to chaos is rather spectacular, and it results in a 'much larger' chaotic attractor than can be found immediately after an accumulation of period-doublings.

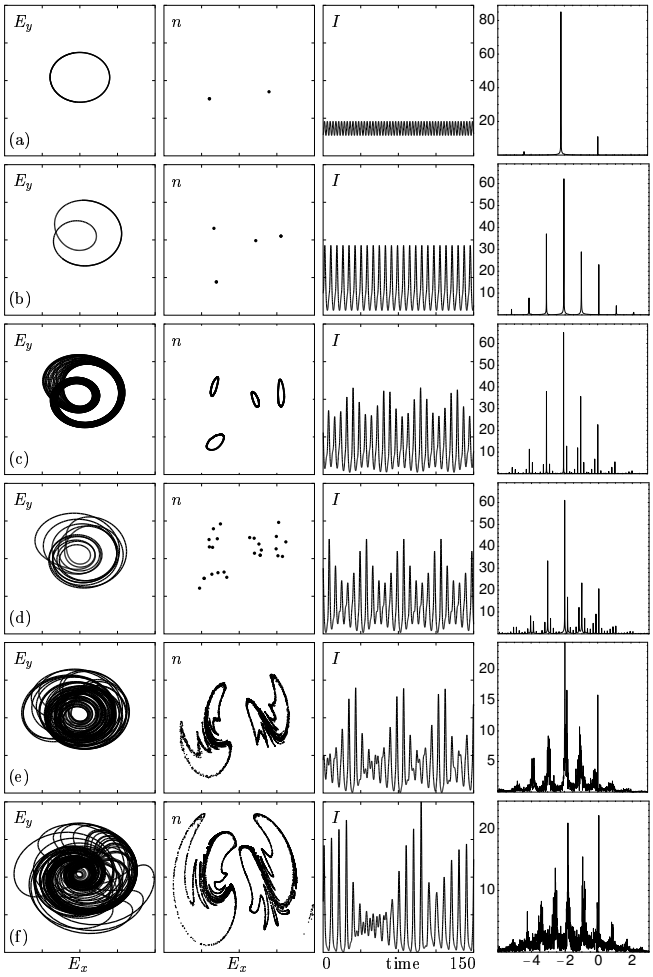

Fig. 4. Transition to chaos via the break-up of a period-two torus; $K = 0.23$ and from (a) to (f) ω takes the values -2.2, -2.0, -1.975, -196, -193, and -1.85.

The two above transitions to chaos can occur in a mixed way. After a number of period-doublings one encounters a torus bifurcation, and the bifurcating torus of some higher base period then breaks up. An example of this is shown in Fig. 4. A periodic orbit (a) loses its stability and a period-two orbit appears (b), which then bifurcates to an attracting torus when the curve T^2 in Fig. 1 (c) is crossed. This torus surrounds the origin twice in projection onto the E-plane, the power is modulated, but the frequencies of the period-doubling are still prominent in the spectrum. The dynamics on the torus then locks to a period-six orbit (d). After the locking the torus is already breaking up (e), which is also clear from the power series and the broadening spectrum. The chaotic attractor then grows, the power series becomes more chaotic and the spectrum even broader. Notice that there is still clear evidence of the frequencies that appeared in the period-doubling.

In summary we identified and mapped out in detail different routes to chaos, namely a sequence of period-doublings, and the break-up of two different tori. The importance of this work lies in providing clear information of where certain types of chaotic dynamics can be found in a laser system that is experimentally quite accessible. In particular, we pointed out different output characteristics of the lasers, corresponding to chaotic attractors born in different ways. The chaotic attractor after period-doublings does not have a very broad spectrum and the frequency peaks typical for period-doubling are still very prominent. These peaks disappear and the spectrum broadens only after a further growth of the attractor. On the other hand, the spectrum after the break-up of a torus appears to be quite broad. Here, a possible pitfall for applications is the occurence of locking on the broken-up torus. We found a loss of chaos over a certain parameter range due to locking onto a period-three orbit. We expect this to be observable in experiments. We remark that avoilding a loss of chaos is particularily important for applications requiring a region of chaotic output that is stable under certain changes in the parameter, such as chaotic encryption schemes where the parameter values provide the encryption key. Investigating this further remains an interesting challenge for future research.

B.K. thanks the British Council for support under the UK-Dutch Joint Scientific Research Programme. The research of S.M.W. was supported by the Foundation for Fundamental Research on Matter (FOM), which is financially supported by the Netherlands Organization for Scientific Research (NWO).

1. G.D. VanWiggeren and R. Roy, *Science* **279** (1997) 1198
2. C.R. Mirasso, P. Colet, and P. Garcia-Fernández, *IEEE Photonics Technology Letters* **8** (2) (1996) 299–301.
3. S. Sinha, W.L. Ditto, *Phys. Rev. Lett.* **81** (10) (1998) 2156–2159.
4. G.H.M. van Tartwijk and D. Lenstra, *Quant. Semiclass. Opt.* **7**, 87 (1995).
5. L.A. Lugiato, L.M. Narducci, D.K. Bandy, and C.A. Pennise, *Opt. Comm.* **46** (1983) 64–68.
6. J.R. Tredicce, F.T. Arecchi, G.L. Lippi, and G.P. Puccioni, *J. Opt. Soc. Am. B* **2** (1) (1985) 173–183.
7. V. Annovazzi-Lodi, S. Donati, and M. Manna, *IEEE J. Quantum Electron.* **30** (7) (1994) 1537–1541.
8. V. Kovanis, A. Gavrielides, T.B. Simpson, and J.M. Liu, *Appl. Phys. Lett.* **67**(19) (1995) 2780-2782.
9. T.B. Simpson, J.M. Liu, K.F. Huang, and K. Tai, *Quant. Semiclass. Opt.* **9** (5) (1997) 765–784.
10. S.M. Wieczorek, B. Krauskopf, and D. Lenstra, *Optics Communications* **172**(1-6) (1999) 279-295.